Published Online First on July 7, 2009 as 10.1158/1535-7163.MCT-09-0122

Upregulation of thrombospondin-1 and angiogenesis in an aggressive human pancreatic cancer cell line selected for high metastasis

Michele K. McElroy,[1] Sharmeela Kaushal,[1] Hop S. Tran Cao,[1] A.R. Moossa,[1] Mark A. Talamini,[1] Robert M. Hoffman,[1,2] and Michael Bouvet[1]

[1]Department of Surgery, University of California, San Diego and [2]AntiCancer, Inc., San Diego, California

Abstract

Pancreatic cancer remains a leading cause of death despite its relatively low incidence. As in many other solid tumors, angiogenesis is critical to the growth and metastasis of this cancer. Through serial in vivo passages in mice, we have developed a highly aggressive variant of human pancreatic cancer cell line XPA-1 which shows more rapid primary tumor growth, faster time to metastasis, and more rapid lethality than the parental cell line. The high-metastatic variant developed a much denser tumor vasculature early during growth within the pancreas. Interestingly, examination of the in vitro growth of this aggressive variant yielded no significant difference from the parental cell line. Real-time PCR evaluation of genes involved in angiogenesis revealed a 24-fold increase in Thrombospondin-1 expression in cells derived from the high-metastatic variant when compared with the parental cell line. These findings provide direct evidence that elevated capability for angiogenesis, mediated by specific changes in gene expression, can lead to a large increase in cancer aggressiveness and resulting metastasis. These findings have important implications for the treatment of metastatic disease. [Mol Cancer Ther 2009;8(7):1779–86]

Introduction

Despite its relatively low incidence in the population, pancreatic adenocarcinoma remains the fourth leading cause of cancer-related death in the United States (1), with overall 5-year survival as low as 5% (2). Recent advances in surgical and critical care have had little impact on the epidemiology of this disease, largely because of its often late stage at presentation (3) and its aggressive biology. The precise mechanisms involved in local tumor progression and metastasis in this disease remain poorly understood. Local invasion and distant metastasis occur within complex tumor-host microenvironments and involve signal exchange between cancer cells and host stroma. The tumor microenvironment promotes proliferation and survival of cancer cells in addition to stimulating cancer cell migration and invasiveness (4). Pancreatic adenocarcinoma, in particular, is characterized by a dense stromal reaction, which has been postulated to support tumor invasion (5).

The oxygen and nutrients that are central to cell survival are supplied to tissues by functioning vasculature. New blood vessel formation (angiogenesis) is critical to continued local and systemic progression of rapidly growing tumors. The formation of new blood vessels is initiated by signaling from cancer and stromal cells, including the release of stimulatory factors, which begin a series of events ultimately leading to endothelial cell degradation of extracellular matrix, migration, and proliferation (6, 7). A number of factors involved in angiogenesis are often perturbed in pancreatic cancer, including upregulation of proangiogenic cytokines (8). Pancreatic cancer has been shown to metastasize via hematogenous spread (9), and clinical studies in patients with pancreatic cancer have linked increased tumor angiogenesis with poorer prognosis (10).

The realization of the critical nature of angiogenesis in tumor growth and metastasis has led to the development of pharmacologic agents that block various steps in the process of tumor neovascularization (11). Growing experience with these drugs has underscored the complex nature of tumor angiogenesis, which involves a dynamic interplay between positive and negative secreted regulators in addition to local tissue modulators (6). Indeed, both pro- and anti-angiogenic mediators may play a role in tumor vasculature maturation and function (12).

We describe here a highly aggressive human pancreatic cancer cell line generated through repeated in vivo passage to select highly metastatic cells, which shows both increased tumor vascularity and upregulation of Thrombospondin-1 (TSP-1), a molecule whose role in angiogenesis remains incompletely understood (13, 14).

Materials and Methods

Cell Culture

Cells were maintained in RPMI 1640 media supplemented with 10% fetal bovine serum (FBS) from Gibco-BRL, Life

Received 2/13/09; revised 5/1/09; accepted 5/1/09; published OnlineFirst 7/7/09.

Grant support: Cancer Therapeutics Training Program (T32 CA121938) (MB); National Institutes of Health (CA109949-03) (MB); American Cancer Society (RSG-05-037-01-CCE) (MB); and National Institutes of Health (CA103563) (AntiCancer Inc.).

The costs of publication of this article were defrayed in part by the payment of page charges. This article must therefore be hereby marked *advertisement* in accordance with 18 U.S.C. Section 1734 solely to indicate this fact.

Requests for reprints: Robert M. Hoffman, AntiCancer, Inc., 7917 Ostrow Street, San Diego, CA 92111. Phone: 858-654-2555; Fax: 858-268-4175. E-mail: all@anticancer.com

doi:10.1158/1535-7163.MCT-09-0122

Technologies, Inc. (Grand Island, NY). The human pancreatic cancer cell line XPA-1 was a gift from Dr. Anirban Maitra at Johns Hopkins University. All media were supplemented with penicillin/streptomycin (Gibco-BRL), L-glutamine (Gibco-BRL), MEM nonessential amino acids (Gibco-BRL), sodium bicarbonate (Cellgro, Herndon VA), and sodium pyruvate (Gibco-BRL). All cell lines were cultured at 37°C with 5% CO_2.

Production of a Stable Red Fluorescent Cell Line (XPA1-RFP)

The pDSRed-2 vector from Clontech Laboratories, Inc. (Palo Alto, CA) was used for stable expression of RFP in the human pancreatic cancer cell line XPA-1. The *Hin*dIII/*Not*I fragment of pDsRed2 (Clontech Laboratories, Inc.) was inserted into the *Hin*dIII/*Not*I site of the pLNCX2 plasmid (Clontech Laboratories, Inc.) containing the neomycin resistance gene to produce the pLNCX2-DsRed2 plasmid. The pLNCX2-DsRed2 plasmids were transfected into PT67 packaging cells using the LipofectAMINE system (Gibco-BRL). Vector production was accomplished via growth in PT67 packaging cells cultured in the presence of 200 to 1,000 μg/mL Geneticin (G418) from Invitrogen Corporation (Carlsbad, CA) for 7 days. Twenty percent confluent XPA-1 cells were incubated with retroviral supernatants of the packaging cells until high levels of DsRed2 expression were observed under fluorescence microscopy. The cells were then harvested and subcultured in selective medium containing G418. The G418 was increased in a stepwise fashion from 200 μg/mL to 2,000 μg/mL. Clones with high DsRed2 expression were isolated and grown for 10 passages in the absence of G418 to select for stable in vitro expression of DsRed2.

Animal Care

Athymic *nu/nu* nude mice and transgenic *nu/nu* mice with the nestin-driven green fluorescent protein (GFP) transgene (which express GFP in nestin-positive tissues; ref. 15), both between 4 and 6 weeks of age, were maintained in a barrier facility on high efficiency particulate air (HEPA)-filtered racks. The animals were fed with autoclaved laboratory rodent diet (Teckland LM-485; Western Research Products, Orange, CA). All invasive procedures and imaging were done with the animals anesthetized by intramuscular injection of 0.02 mL of a solution of 50% ketamine, 38% xylazine, and 12% acepromazine maleate. All surgical procedures were done under sterile conditions. All animal studies were conducted in accordance with the principles and procedures outlined in the National Institutes of Health (NIH) Guide for the Care and Use of Animals under Assurance number A3873-01.

Orthotopic Implantation of Pancreatic Tumors

Human pancreatic cancer xenografts from the pancreatic cancer cell line XPA1-RFP were established in nude mice by surgical orthotopic implantation (SOI), a procedure developed in our laboratory (16). Briefly, small subcutaneous tumors were initiated in 4- to 6-week-old female *nu/nu* mice via subcutaneous injection of 1×10^6 XPA1-RFP cells into the left flank. When these tumors reached approximately 1 cm diameter, the animals were euthanized and the tumor was harvested and sectioned into 1-mm^3 pieces. Recipient 4- to 6-week-old female *nu/nu* mice were then anesthetized as described, and a small transverse incision was then made in the left lateral flank through the skin and peritoneum. The tail of the pancreas was exposed, and a 1-mm^3 piece of tumor tissue was sutured into the pancreatic tail using 8-0 nylon surgical sutures from US Surgical (Norwalk, CT). The pancreas was then returned to the abdomen, and the peritoneum and skin were closed using 6-0 polysorb surgical sutures (US Surgical).

Establishing the High Metastatic Variant

Orthotopic human pancreatic cancer xenografts from the pancreatic cancer cell line XPA1-RFP were initially established in nude mice by SOI as described above. These tumors were allowed to grow until the animals developed widespread metastases and malignant ascites. At the time of sacrifice, the ascitic fluid was harvested and placed on ice. Four- to 6-week-old female *nu/nu* mice were anesthetized and a small transverse incision was made in the left lateral flank through the skin and peritoneum. The tail of the pancreas was exposed, and 50 μL of malignant ascites were injected into the pancreatic tail. The pancreas was then returned to the abdomen, and the peritoneum and skin were closed using 6-0 polysorb surgical sutures (US Surgical). After six serial passages in this fashion, the resulting primary tumor and malignant ascites were harvested. The primary tumor and malignant ascites were gently dissociated and plated for in vitro culture. After a single in vitro passage for expansion, the passage-6 ascites and passage-6 primary cells were stored in liquid nitrogen for later analysis.

Animal Imaging

Mice were imaged using the Olympus OV100 Small Animal Imaging System (Olympus Corp., Tokyo, Japan), containing an MT-20 light source (Olympus Biosystems Planegg, Germany) and DP70 CCD camera (Olympus Corp.) on the basis of the expression of fluorescent proteins, a procedure developed in our laboratory (17, 18). All images were analyzed using Image-J (NIH, Bethesda, MD) and were processed for contrast and brightness with the use of Photoshop element-4 (Adobe Systems Inc., San Jose, CA).

Blood Vessel Measurement

Tumors harvested from nestin-GFP mice, which express GFP nude in nascent blood vessels, as established by our laboratory (15), were weighed and measured for volume and gently compressed between two glass slides as previously described (19). Sequential images at high magnification using the GFP narrow bandpass filter were obtained with the OV100 Small Animal Imaging System. All GFP-expressing blood vessels were measured using Image-J software and calculated as blood vessel density (blood vessel length/tumor volume = mm/mm^3). Tumor volume was calculated as length × height × width × 0.52.

Histology

Primary and metastatic tumor samples were removed en bloc with surrounding tissue at the time of sacrifice, fixed in Bouin's Solution, and embedded in paraffin prior to sectioning and staining with hematoxylin and eosin (H&E) for standard light microscopy. All slides were imaged using

Table 1. Gene expression in the high-metastatic variant

Type of Gene	Fold Difference (P6/P0)					
	0.1–0.5	0.5–1.0	1.0–2.0	2.0–10	10–20	>20
Angiogenic factors	*VEGFC*	*PGF*	*ANGPT 1*	*ANPEP*		
		STAB1	*ANGPT 2*	*EREG*		
		VEGF A	*FGF1*	*IL8*		
			TYMP			
			FGF_2			
			FIGF			
			FLT_1			
			JAG_1			
			KDR			
			LAMA5			
			NRP1			
			NRP2			
			PLXDC1			
Adhesion molecules			*ANGPTL3*			
			BAI 1			
			COL4A3			
Proteases, inhibitors, and other molecules		*ANGPT4*	*PECAM1*			
			PF4			
			PROK2			
			SERPINF1			
			TNFAIP2			
Transcription factors and others			*HAND2*			
			SPHK1			
Other factors involved in angiogenesis						
Cytokines and chemokines	*CXCL10*	*CXCL9*	*CCL11*	*CXCL1*		
	IFNB1	*IFNA1*	*CCL2*			
		IL6	*CXCL3*			
		MDK	*CXCL5*			
		TNF	*CXCL6*			
Other growth factors and receptors		*HGF*	*EFNA1*	*EGF*	*EDG_1*	
		ITGB3	*EFNA3*			
		TGFBR1	*EFNB2*			
			EPHB4			
			FGFR3			
			IGF1			
			PDGFA			
			TEK			
			TGFA			
			TGFB1			
			TGFB2			
Adhesion molecules		*ITGB3*	*CDH5*			*TSP*
			COL18A1			
			ENG			
			ITGAV			
			THBS2			
Protease inhibitors and other matrix proteins	*TIMP2*	*LECT1*	*LEP*	*PLAU*		
			MMP2			
			MMP9			
			PLG			
			TIMP1			
			TIMP3			
Transcription factors and others			*AKT1*	*HPSE*		
			HIF1A	*ID3*		
			NOTCH 4	*ID1*		
			PTGSI1			

NOTE: Multiple genes involved in angiogenesis, including growth factors and receptors, adhesion molecules, proteases, matrix proteins, and transcription factors, were evaluated for expression using real-time PCR via the RT^2 Profiler PCR Array System. The table lists the genes of interest evaluated and their fold increase or decrease in the high-metastatic variant as compared with the parental cell line. In contrast to many of the angiogenesis-related genes evaluated, TSP-1 showed a 24-fold increase in expression in the high-metastatic variant. Complete abbreviations of genes can be found at http://www.sabiosciences.com/.

an inverted Nikon DE-300 microscope and Spot camera RD. All images were analyzed using Image-J and were processed for contrast and brightness with the use of Photoshop element-4.

In vitro Proliferation

All cell lines evaluated were thawed from frozen stocks and assayed within two passages after thaw. The aggressive (generated from either primary tumor or malignant ascites) and parental cell lines (XPA1-RFP) were plated in 96-well plates in triplicate at 5,000 cells per well. Four days later, proliferation was quantified using an XTT assay from Biotium Inc. (Hayward, CA). The XTT developing reagent was added to the wells and allowed to incubate for 4 hours at 37°C. Plates were then read using a standard plate reader at OD 490 nm. OD readings between the three cell lines were evaluated by ANOVA using NCSS Statistical Software (Kaysville, UT) for statistically significant differences in cell proliferation.

RNA Isolation from Cultured Cells

Total RNA was isolated from the high-metastatic and parental cell lines using the RNeasy kit from Qiagen (Valencia, CA). Briefly, cells were grown in RPMI as described. At 75% confluence, the cells were scraped from the dish, washed once using ice-cold phosphate buffered saline (PBS) from Gibco-BRL, and counted. The cells were then pelleted and homogenized. An equal volume of 70% ethanol was added to the homogenized lysate, and the mixture was applied to an RNeasy midi-spin column. The RNA was washed several times while on the column according to the manufacturer's instructions and eluted using RNAse-free water. Total RNA concentration and purity in the eluted samples obtained was quantitated using a

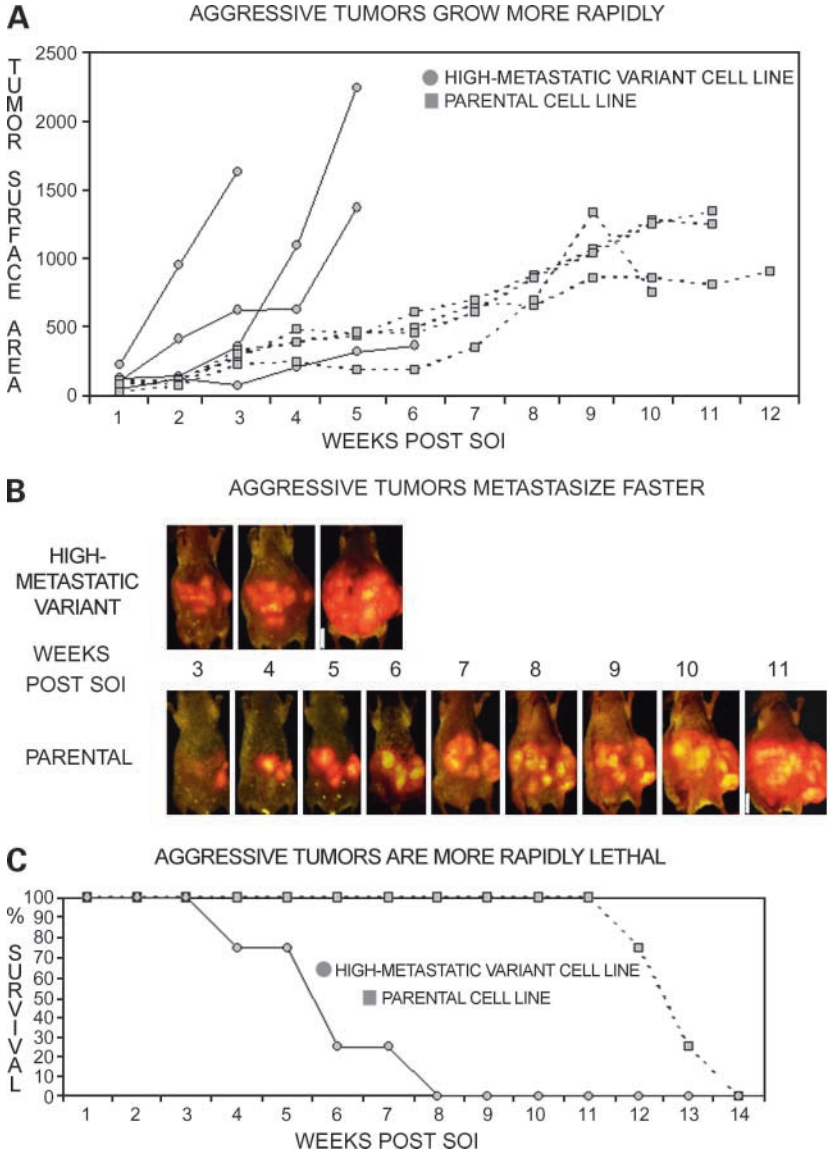

Figure 1. Malignant ascites were isolated from tumor-bearing animals and serially passaged into the pancreas of 4- to 6-week-old female *nu/nu* mice. The aggressive high-metastatic variant grew more rapidly in vivo and was more rapidly lethal than the parental cell line XPA1-RFP. Measurement of tumor surface area (measured in mm^2) via whole-body imaging showed much more rapid primary growth of tumors generated from the high-metastatic variant cell line. **A,** representative animals from each group imaged using the Olympus OV-100 show the earlier time to widespread metastasis in the aggressive variant. **B,** survival data from each group show more rapid mortality in animals bearing tumors from the aggressive variant. **C,** the solid line indicates growth of tumors in animals implanted with the aggressive variant, whereas the dotted line represents the parental line.

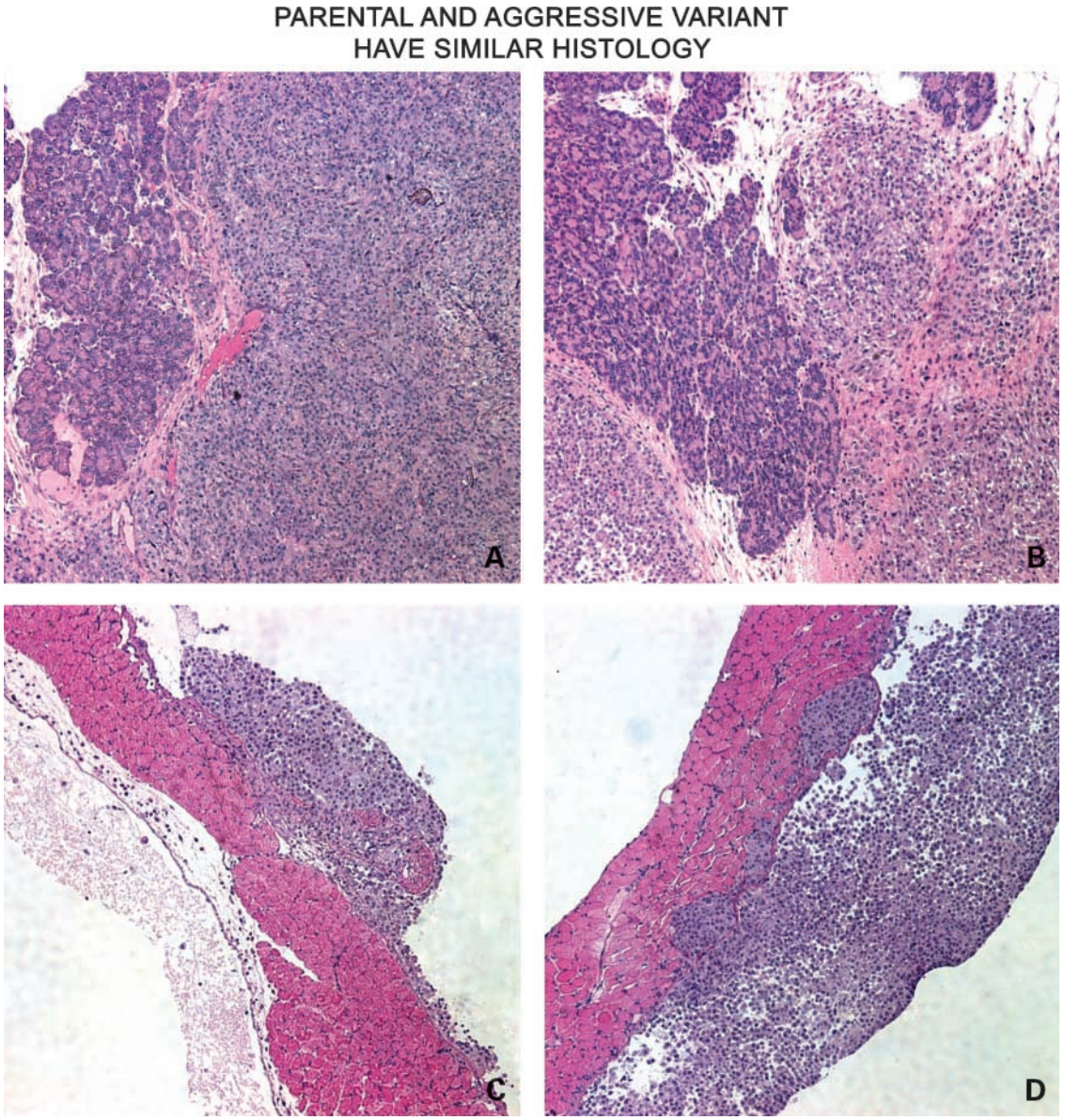

Figure 2. The aggressive-variant and parental tumors show similar histology. Tumors generated from the parental and aggressive-variant cell lines were harvested and evaluated using light microscopy. Primary tumors from the parental cell line. **A,** and the aggressive-variant cell line, **B**, were virtually indistinguishable by light microscopy. Likewise, diaphragmatic metastases from the parental cell line, **C**, and the aggressive-variant cell line, **D**, showed very similar histology.

NanoDrop ND-100 UV spectrophotometer from NanoDrop Technologies, LLC (Wilmington, DE).

cDNA Preparation

Following RNA preparation, the samples were treated with DNase to ensure elimination of genomic DNA, and the extracted RNA was converted to cDNA using the RT^2 First Strand Kit from SuperArray Bioscience Corporation (Frederick, MD). Briefly, 25 to 50 ng RNA was combined with 2 μL genomic DNA-elimination buffer and brought up to a final volume of 10 μL using RNAse-free H_20. This mixture was incubated at 42°C for 5 minutes, then chilled on ice. Ten microliters of RT Cocktail was then added to this mixture and incubated at 42°C for exactly 15 minutes followed by 5 minutes at 95°C. Ninety-one microliters ddH20 was added to each 20 μL cDNA synthesis reaction, and the diluted cDNA mixture was stored at −20°C until used for gene expression profiling.

Gene Expression Profiling

The RT^2 Profiler PCR Array System (SuperArray, Bioscience Corp.) was used to evaluate the aggressive and parental cell lines for differential gene expression. The genes evaluated in this PCR array include multiple genes involved

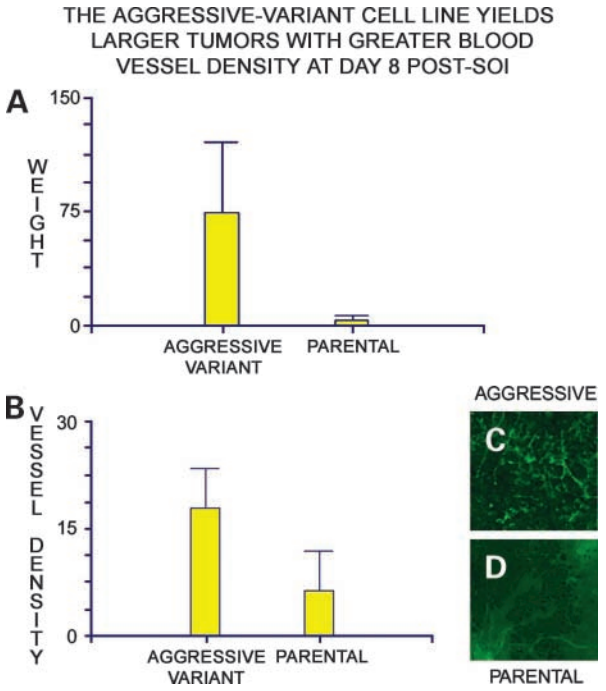

Figure 3. Tumors generated from the aggressive-variant and parental cell lines were implanted into the pancreas of nestin-GFP *nu/nu* mice and allowed to grow for 8 d. At 8 d postimplantation, the tumors were harvested, weighed, and imaged. Tumors from the aggressive variant were significantly larger at day 8. All tumor weights are measured in mg, **A** (P = 0.016 by paired t test). Tumors from the aggressive-variant cell line showed significantly greater density of GFP-expressing nascent blood vessels at day 8. Tumor blood vessel density was measured in mm/mm^3, **B** (P = 0.009 by paired t test). Representative images from aggressive-variant, **C,** and parental, **D,** tumors illustrate the difference in blood vessel density.

in angiogenesis and vascular homeostasis (Table 1). Real-time PCR detection was carried out per the manufacturer's instructions. The experimental cocktail was prepared by adding 550 μL of the SuperArray RT^2 qPCR master mix and 448 μL ddH_20 to 102 μL of the diluted cDNA mixture. For real-time PCR detection, 10 μL of this cocktail was added to each well of the 384-well PCR array. The array was then cycled on a real-time thermal cycler through the following program: 1 cycle of 10 minutes at 95°C followed by 40 cycles of 15 seconds at 95°C and of 1 minute at 60°C. SYBR Green fluorescence was detected from each well during the annealing step of each cycle. Values were exported to a template Excel file for analysis. Analyses of the raw data were done through the Superarray Data Analysis Web Portal (SuperArray Bioscience Corp.).

Results and Discussion

Serial in vivo passage of malignant ascites from human pancreatic cancer-bearing *nu/nu* mice was used to generate a highly aggressive passage-6 generation cell line with much more rapid primary tumor growth and faster time to distant metastasis. The tumors generated from the parental cell line XPA1-RFP grew slowly (Fig. 1A) with eventual metastasis to multiple extra-pancreatic sites. Mice bearing these tumors showed widespread metastasis 9 to 12 weeks after implantation (Fig. 1B) and died within 12 to 14 weeks (Fig. 1C). Repeated in vivo passage of malignant ascites from XPA1-RFP tumor-bearing mice into the pancreas of recipient nude mice yielded a much more aggressive cell line. Tumors generated from the aggressive variant grew rapidly (Fig. 1A) and showed widespread metastasis within 3 to 5 weeks (Fig. 1B). Time to death in this group was from 3 to 8 weeks (Fig. 1C).

Orthotopic parental and aggressive-variant tumors metastasized to distant sites in a similar distribution and yielded histologically similar lesions. Mice bearing tumors generated from the parental cell line XPA1-RFP developed lesions in the liver, spleen, abdominal lymph nodes, mesentery, and lung by 9 to 12 weeks after implantation. Similarly, the aggressive variant metastasized to liver, spleen, abdominal lymph nodes, mesentery, and lung. Whereas the metastatic lesions in the animals bearing tumors from the aggressive variant were found in the same distribution as their parental line, they developed much more rapidly than tumors generated from the parental cell line, within 3 to 5 weeks of tumor implantation. Microscopic evaluation of the metastatic and primary tumors from animals after implantation of either the parental or aggressive-variant cell lines revealed lesions that were histologically indistinguishable (Fig. 2).

In addition to faster growth in vivo, tumors from the aggressive cell line had greater blood vessel density at 8 days after implantation. Cells generated from the aggressive variant were assayed for their early in vivo growth and angiogenesis within the pancreas of transgenic nude mice with

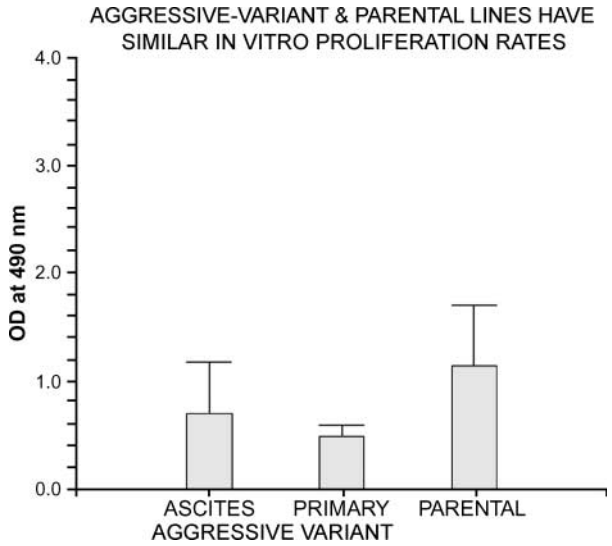

Figure 4. Cell lines derived from the aggressive variant show similar *in vitro* proliferation when compared with the parental cell line (XPA1-RFP). *In vitro* proliferation was evaluated under standard culture conditions using an XTT assay. No significant difference was seen when cell lines derived from either the primary tumor or the malignant ascites derived from an animal implanted with the aggressive variant were compared with the parental cell line XPA1-RFP. Comparison between the three groups was determined by ANOVA (P = 0.15).

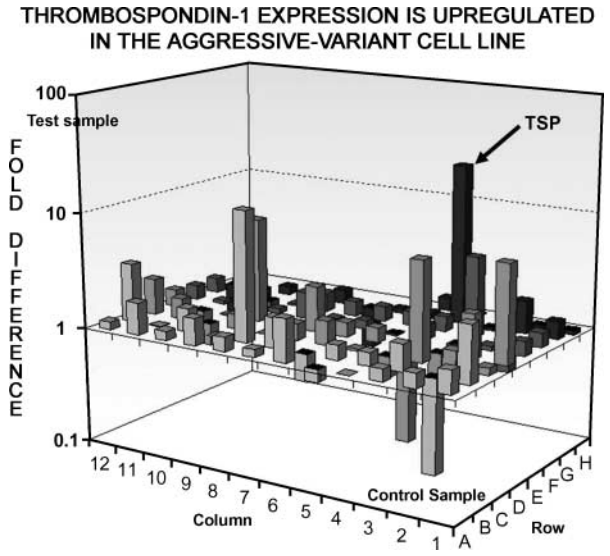

Figure 5. The aggressive variant showed increased TSP-1 expression at the RNA level. Cells derived from the aggressive variant and cells from the parental cell line were harvested and RNA was isolated. The RNA expression of a number of genes involved in angiogenesis was then quantified using real-time PCR. TSP-1 expression was increased 24-fold when compared with the parental cell line (arrow). All bars represent expression in the aggressive cell line divided by expression in the parental cell line (P6/P0).

nestin-driven GFP in which nascent blood vessels express GFP. At 8 days after implantation, tumors generated from the parental cell line were harvested and compared with those generated from the aggressive variant. The aggressive tumors showed more rapid early growth (Fig. 3A) and a greater density of nascent blood vessels within the developing tumor (Fig. 3B-D).

Cell lines generated from the aggressive variant show comparable in vitro morphology and proliferation when compared with the parental cell line. In vitro testing of cell proliferation yielded no significant difference between the parental cell line and cell lines derived from either the primary tumor or malignant ascites of the aggressive variant (Fig. 4).

Evaluation of gene expression showed elevated levels of TSP-1 expression in the aggressive variant. After a single passage in vitro, RNA was harvested from both the parental (XPA1-RFP) and the aggressive variant. Real-time reverse transcriptase (RT)-PCR was used to assay for multiple angiogenic factors including growth factors and receptors, adhesion molecules, proteases, matrix proteins, and transcription factors (Table 1). Upregulation of TSP-1 was shown in cells from the aggressive variant with a 24-fold increase in TSP-1 RNA compared with the parental cell line (Table 1, Fig. 5). Other genes showed no remarkable changes in the variant.

Multiple-passage selection of ascites of the human pancreatic cancer cell line XPA1-RFP has thereby yielded a population of cells with highly aggressive in vivo growth and metastasis. Although this aggressive variant grew faster within the pancreas of living animals and metastasized earlier to distant sites, the cell line generated from this variant did not grow more rapidly in culture. This suggested that the aggressive nature of this variant was related to something other than increased cell proliferation, and the adaptations responsible for its aggressive in vivo behavior may be related to the pancreatic microenvironment present within the living animal. Indeed, evaluation of early orthotopic tumors generated from the aggressive-variant and parental cell lines revealed larger tumors at 8 days postimplantation with greater blood vessel density in the aggressive tumors. Interestingly, real-time PCR evaluation of cells from this aggressive variant showed a 24-fold increase in TSP-1 RNA expression when compared with the parental, less aggressive, cell line.

TSP-1 is a trimeric 450-kDa glycoprotein present in platelets and the extracellular matrix. This protein participates in platelet aggregation as well as in the tissue response to injury (20, 21). The role of TSP-1 in angiogenesis has been somewhat controversial, with both stimulatory and inhibitory functions reported (13, 14, 22, 23). Qian and colleagues found that bovine aortic endothelial (BAE) cell tube formation was enhanced by low levels of TSP-1 but inhibited at higher levels (14). TSP-1 mediated this effect on tube formation through the upregulation of matrix metalloproteinase-9 (MMP-9) in the BEA cells. Nicosia and colleagues showed that matrix-bound TSP-1 was able to promote growth of microvessels and fibroblast-like cells in culture in a dose-dependent fashion (22). TSP-1 has also been shown to be involved in platelet-stimulated smooth muscle proliferation (24), which may play a role in vascular remodeling. Our results suggest an important role for TSP-1 in elevated angiogenesis and metastasis. These findings have important implications for the treatment of metastatic disease.

Future experiments will evaluate protein expression of TSP-1 in the aggressive-variant cell line as compared with both the parental cell line and normal pancreatic tissue, as well as gene and protein expression of TSP-1 in tumors growing within the mouse pancreas. In addition, the time-dependent induction of TSP-1 during tumor development and metastasis will be evaluated, as will the effect of in vitro and in vivo downregulation of the TSP-1 gene.

Disclosure of Potential Conflicts of Interest

No potential conflicts of interest were disclosed.

References

1. Jemal A, Siegel R, Ward E, Murray T, Xu J, Thun MJ. Cancer statistics, 2007. CA Cancer J Clin 2007;57:43–66, PubMed doi:10.3322/canjclin.57.1.43.

2. Yeo C, Yeo T, Hruban R, editors. Cancer of the pancreas. 7th ed. Philadelphia: Lippincott Williams & Wilkins; 2004.

3. Sener SF, Fremgen A, Menck HR, Winchester DP. Pancreatic cancer: a report of treatment and survival trends for 100,313 patients diagnosed from 1985–1995, using the National Cancer Database. J Am Coll Surg 1999;189:1–7, PubMed doi:10.1016/S1072–7515(99)00075-7.

4. Hanahan D, Weinberg RA. The hallmarks of cancer. Cell 2000;100:57–70, PubMed doi:10.1016/S0092-8674(00)81683-9.

5. Qian LW, Mizumoto K, Maehara N, et al. Co-cultivation of pancreatic

cancer cells with orthotopic tumor-derived fibroblasts: fibroblasts stimulate tumor cell invasion via HGF secretion whereas cancer cells exert a minor regulative effect on fibroblasts HGF production. Cancer Lett 2003;190:105–12, PubMed doi:10.1016/S0304-3835(02)00517-7.

6. Gasparini G. The rationale and future potential of angiogenesis inhibitors in neoplasia. Drugs 1999;58:17–38, PubMed doi:10.2165/00003495-199958010-00003.

7. Beckermann BM, Kallifatidis G, Groth A, et al. VEGF expression by mesenchymal stem cells contributes to angiogenesis in pancreatic carcinoma. Br J Cancer 2008;99:622–31, PubMed doi:10.1038/sj.bjc.6604508.

8. Yamanaka Y, Friess H, Buchler M, et al. Overexpression of acidic and basic fibroblast growth factors in human pancreatic cancer correlates with advanced tumor stage. Cancer Res 1993;53:5289–96, PubMed.

9. Kamisawa T, Isawa T, Koike M, Tsuruta K, Okamoto A. Hematogenous metastases of pancreatic ductal carcinoma. Pancreas 1995;11:345–9, PubMed doi:10.1097/00006676-199511000-00005.

10. Karademir S, Sokmen S, Terzi C, et al. Tumor angiogenesis as a prognostic predictor in pancreatic cancer. J Hepatobiliary Pancreat Surg 2000;7:489–95, PubMed doi:10.1007/s005340070020.

11. Homsi J, Daud AI. Spectrum of activity and mechanism of action of VEGF/PDGF inhibitors. Cancer Control 2007;14:285–94, PubMed.

12. Fukumura D, Jain RK. Tumor microvasculature and microenvironment: targets for anti-angiogenesis and normalization. Microvasc Res 2007;74:72–84, PubMed doi:10.1016/j.mvr.2007.05.003.

13. Volpert OV. Modulation of endothelial cell survival by an inhibitor of angiogenesis thrombospondin-1: a dynamic balance. Cancer Metastasis Rev 2000;19:87–92, PubMed doi:10.1023/A:1026560618302.

14. Qian X, Wang TN, Rothman VL, Nicosia RF, Tuszynski GP. Thrombospondin-1 modulates angiogenesis *in vitro* by up-regulation of matrix metalloproteinase-9 in endothelial cells. Exp Cell Res 1997;235:403–12, PubMed doi:10.1006/excr.1997.3681.

15. Amoh Y, Yang M, Li L, et al. Nestin-linked green fluorescent protein transgenic nude mouse for imaging human tumor angiogenesis. Cancer Res 2005;65:5352–7, PubMed doi:10.1158/0008-5472.CAN-05-0821.

16. Hoffman RM. Orthotopic metastatic mouse models for anticancer drug discovery and evaluation: a bridge to the clinic. Invest New Drugs 1999;17:343–59, PubMed doi:10.1023/A:1006326203858.

17. Chishima T, Miyagi Y, Wang X, et al. Cancer invasion and micrometastasis visualized in live tissue by green fluorescent protein expression. Cancer Res 1997;57:2042–7, PubMed.

18. Hoffman RM. The multiple uses of fluorescent proteins to visualize cancer *in vivo*. Nat Rev Cancer 2005;5:796–806, PubMed doi:10.1038/nrc1717.

19. Amoh Y, Li L, Tsuji K, et al. Dual-color imaging of nascent blood vessels vascularizing pancreatic cancer in an orthotopic model demonstrates antiangiogenesis efficacy of gemcitabine. J Surg Res 2006;132:164–9, PubMed doi:10.1016/j.jss.2005.12.028.

20. Lawler JW, Slayter HS, Coligan JE. Isolation and characterization of a high molecular weight glycoprotein from human blood platelets. J Biol Chem 1978;253:8609–16, PubMed.

21. Raugi GJ, Olerud JE, Gown AM. Thrombospondin in early human wound tissue. J Invest Dermatol 1987;89:551–4, PubMed doi:10.1111/1523–1747.ep12461198.

22. Nicosia RF, Tuszynski GP. Matrix-bound thrombospondin promotes angiogenesis *in vitro*. J Cell Biol 1994;124:183–93, PubMed doi:10.1083/jcb.124.1.183.

23. Sharghi-Namini S, Fan H, Sulochana KN, et al. The first but not the second thrombospondin type 1 repeat of ADAMTS5 functions as an angiogenesis inhibitor. Biochem Biophys Res Commun 2008;371:215–9, PubMed doi:10.1016/j.bbrc.2008.04.047.

24. Ichii T, Koyama H, Tanaka S, et al. Thrombospondin-1 mediates smooth muscle cell proliferation induced by interaction with human platelets. Arterioscler Thromb Vasc Biol 2002;22:1286–92, PubMed doi:10.1161/01.ATV.0000024684.67566.45.